Label-Free Investigation of Yeast Cell Physiology in Capillary Tubes Sensed by THz Waves

V. Matvejev[1], F. Ielasi[2], C. De Tandt[1], W. Ranson[1], R. Willaert[2], J. Stiens[1]
Laboratory of Micro- and Photoelectronics, LAMI-ETRO[1]; Laboratory of Structural Biology[2]
Vrije Universiteit Brussel,
Pleinlaan 2, Brussels, 1050 Belgium

***Abstract*—For autonomous cell population evolution in space monitoring with THz absorption spectroscopy a micromachined sensor prototype was developed. The first measurements on *Saccharomyces cerevisiae* cell detection are presented.**

I. Introduction

Due to their specific nature, THz waves are able to probe different states of bio-material (e.g. DNA, protein, cell) and the different states of water molecules (hydration shells, water contained within a cell, fast and slow water) associated with it[1]. However sensing solutes in liquids, which has a significant number of potential applications including label-free sensing, is limited by technological challenges.

Bulk water as a highly polar liquid induces strong attenuation and shadows the response of analyte, we are interested in. We attempt to overcome this downside by a sensor configuration whereby we target maximum interaction between the generated THz wave and the analyte material present in a capillary tube with liquid. To show the application of this sensor prototype we present the detection of a cell population state.

As a model system to study the effect of microgravity conditions on cell physiology, we selected the eukaryotic microorganism *S. cerevisiae*. This tractable and harmless microorganism offers important advantages for microbial physiology research in microgravity, such as its GRAS (Generally Recognized as Safe) classification and powerful genetic tools. It has been shown that growth of *S. cerevisiae* under microgravity conditions results in strain-dependent microgravity stress [2]. Microgravity conditions disturbed spatially programmed budding patters and generated strain-dependent growth differences in yeast colonies on semi-solid medium.

In this paper we will present the design of the THz sensor prototype, based on micromachined waveguides in silicon. The sensitivity of the sensor is investigated with a FEM model. The first experiments on the cell growth detection with integrated THz are reported.

II. Measurement Methods

The sensor prototype was modeled. Three cell populations were investigated. They were contained within a capillary tube inserted through a micromachined waveguide and the scattering parameters of the waveguide and capillary cube (CT) arrangement were measured.

A. Micromachining

Waveguides operating at low THz frequency range (100–1100 GHz) and with cross-section dimensions scaling from $1500\,\mu\mathrm{m}$ down to $150\,\mu\mathrm{m}$ have to be achieved with demanding accurate dimensional control and high tolerances to achieve VSWR=1.1 of coupling structures and transitions, low surface roughness to restrain excessive losses. All this requirements can be achieved with photolithography and deep anisotropic wet etching of <100> Si in KOH solution, resulting in trenches with sloped side walls under the precise angle of $54.74°$. After producing the trenches, metalization (evaporation and plating) and cleaving/dicing, the mirrored split-blocks are then aligned with a flip-chip and bonded by thermo-compressive bonding. This approach results in enclosed high quality waveguides [3] and cavities, with hexagonal cross-section. By means of pre-etch masks patterns designed to expose the crystalline orientation and additional etching the underetch was reduced to average of $8\,\mu\mathrm{m}$, which can be compensated during the design. The additional cleaving grooves were added to the design to increase yield and accuracy of the cleaving process. Corner compensation by <100> oriented combs results in negligibly underetched convex corners. By introducing patterns on the backside of the wafer, the holes were made to pass through off-the-plane capillary tubes in the center of hexagonal waveguide (WH).

B. Modeling

Microwave Studio from CST was used to model the response of the THz sensor arrangement. The sensor was modeled as an air filled WH made in a gold block centered between two WR3.4 waveguides (see fig. 1). It was decided to implement waveguides with slightly larger dimensions than needed for an optimal coupling between WR3.4-WH. Larger WH dimensions reduce the demand for accurate alignment and a good mechanical contact/fix at the expense of lower coupling efficiency. The WH with $1200\,\mu\mathrm{m}$ width and $500\,\mu\mathrm{m}$ height with the length of $10\,\mathrm{mm}$ was modeled for subsequent implementation. Various polyvinyl coated silica CT (from Polymicro Technologies) were modeled, the CT were inserted through appropriate sized openings in the chip.

The electromagnetic properties of studied cells were unknown, however the expected characteristics of their solution should be very close to water, since only a small amount of cells is present in water and cells contain biological water. Therefore the sensitivity of the arrangement to Liquid Under

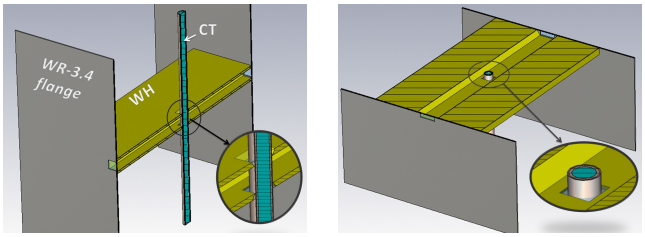

(a) (b)

Fig. 1. Sensor model, longitudinal-vertical (a) and -horizontal (b) cuts.

Test (LUT) was studied by deviating its dielectric permittivity from values given for pure water given in [4]. The difference in scattering parameters was defined as the sensitivity of the device to a certain dielectric permittivity change (e.g. $dB/(0.2\Delta\epsilon \cdot \epsilon^{-1})$) and the design parameters were optimized to find the highest sensitivity. Naturally the CT with largest internal diameter and smallest external diameter gave more sensitivity together with larger attenuation. This was confirmed by measuring two capillaries with $150\,\mu\mathrm{m}$ and $320\,\mu\mathrm{m}$ of internal diameters filled with water and then water/methanol solutions (not presented here).

C. Sample Preparation

Cells were cultivated overnight at $30\,^{\circ}\mathrm{C}$, centrifuged, washed 2 times with phosphate buffered saline (PBS) solution and resuspended in a small volume of the same buffer. Afterwards the total cell population was equally divided into three parts. One cell population was left as it was, a second one was treated thermally at $70\,^{\circ}\mathrm{C}$ for $10'$ and into the third population $1\,\mathrm{mg/ml}$ sodium azide (NaN_3 – toxic material) was added. The two treatments were carried out in order to kill the cells in two different ways. The heat-killed cells loose their plasma membrane integrity, although the cell's morphological characteristics are maintained [5], [6]. The difficulty in measuring cells was their tendency to precipitate (segment, sink) with time due to gravity if left unstirred, this required a steady flow and short-time measurements.

D. Measurement Setup

In fig. 2 the measurement setup is shown, the generated THz wave is coupled to WH&CT and the reflected wave is detected with reflection detector via the Directional Coupler (DC). The THz-wave transmitted through WH&CT is coupled to the Transmission Detector. The coupling from standardized WR-3.4 waveguide with a flange to Si-chip with WH (no flange) was done by butt-coupling of the aligned WH to WR. The WH is placed on $XYZ\Theta$-μpositioning stage, allowing precise alignment with respect to the source and detection flanges. The detection part is placed on an x-positioning stage, allowing to bring WH into contact with the flanges. The position of the WH considered to be optimal when the maximal transmission was achieved at several frequencies. Then WH was fixed by applying moderate amount of pressure with the transmission detector on the x-positioning stage. Once the WH is fixed a CT can be inserted through the WH and a syringe fixed to

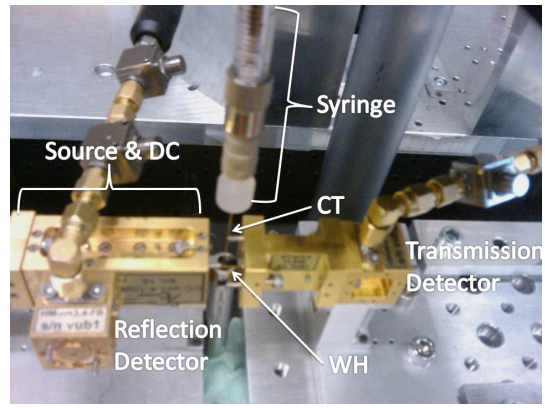

Fig. 2. Measurement setup.

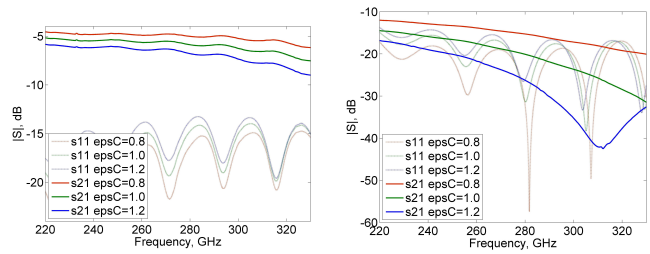

(a) (b)

Fig. 3. Simulated S-parameters for the structure with CT $r_{int} = 150\,\mu\mathrm{m}$ and $r_{ext} = 363\,\mu\mathrm{m}$ internal and external diameters (a); $r_{int} = 320\,\mu\mathrm{m}$ and $r_{ext} = 435\,\mu\mathrm{m}$ diameters (b).

it. The syringe can be refilled, by removing its plunger with piston from the fixed barrel with attached CT.

III. Results

In order to find best sensitivity with a given sensor arrangement the scattering parameters for different CT were simulated. For a given WH working in the 220–325 GHz frequency range, it was found that a CT with internal and external diameter of $320\,\mu\mathrm{m}$ and $435\,\mu\mathrm{m}$, respectively, yields the highest sensitivity without degrading transmitted signal. The S-parameters of two cases are shown in fig. 3, where CT with smaller internal diameter induces smaller changes in S-parameters. However, bigger CT would impose requirement on higher dynamic range of the measurement system. It was also noticed that transmission signal changes more than reflection.

Visualizing the calculated EM-field distributions allows to study the electric field distributions of the propagating THz wave and interactions with the LUT. The field reflects strongly on the CT and hence only partially interacts with the LUT. This penetration, however, concentrates along the internal CT/LUT interface.

The first approach to measure and detect the changes in S-parameters for WH/CT arrangement loaded with different LUTs was by injecting the LUT and doing frequency sweep with a large step (21 frequency point) and high number of averaging, motivated by tendency of the sample to segment and expectancy of signal changes comparable to detection

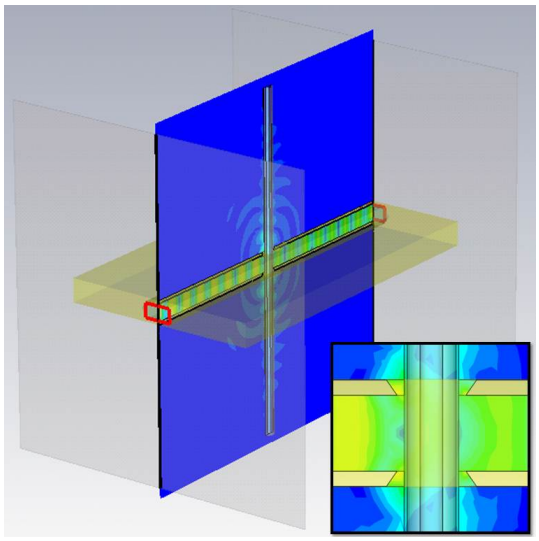

(a)

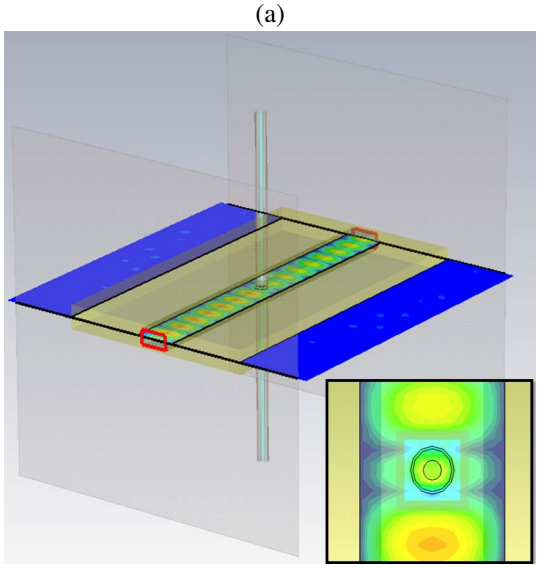

(b)

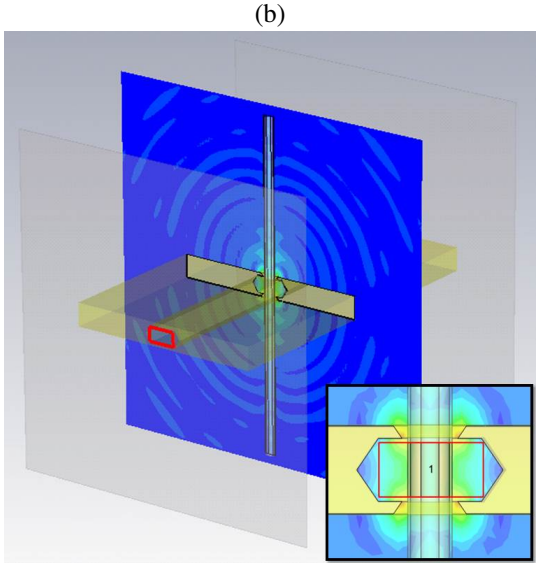

(c)

Fig. 4. Simulated field distributions along x- (a), y- (b), z-axis (c). Magnification on the CT in the inset.

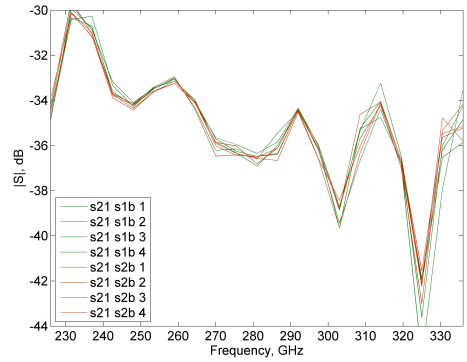

Fig. 5. Frequency sweep transmission measruements on the *S. cerevisiae*.

TABLE I
TIME SWEEP AT 275GHZ, THE TRANSMISSION RANGES FOR DIFFERENT SAMPLES.

S#	Treatment	Resuspended	min($\|S_{21}\|$)	max($\|S_{21}\|$)
s1a	No	No	29.47	29.82
s1b	No	Yes	29.56	30.15
s2a	Thermal	No	27.38	28.15
s2b	Thermal	Yes	26.81	28.00
s3a	Toxic	No	28.35	28.92
s3b	Toxic	Yes	28.08	28.60
s3a	Toxic	No	28.58	28.92

noise. This approach did not gave any useful result, see fig. 5. All the curves seemed to overlay each other with some random noise added. But the second approach of injecting the LUT while performing the time sweep at one frequency gave a clear transmission amplitude difference for different LUTs (see fig. 6). In total, seven samples were measured with time sweep, the samples marked with letter *a* where not resuspended, that is when the sample was segmented the denser layer of cells on the bottom of the container was collected and injected into the capillary. This way *a*-type samples where more dense but concentration was different from sample to sample. The important derived measurement data values presented in the table I.

IV. DISCUSSIONS

The sample quantities used during the measurements were on the order of $100\,\mu$l and operating with the samples was not trivial task, due to its viscosity and tendency to segment. After re-suspending the cells and applying the sample in to the syringe some air-bubbles/pockets were formed preventing the homogeneous sample flow through the capillary. This can be seen as added noise and if averaged adds some randomness during the frequency measurements, with time-sweep scans at one frequency it is easy to observe this deviations in the form of sudden increase in transmitted power (tiny air bubble reduces the attenuation) and thus can be discarded.

From the measured data we see that sample 1 with living cells has the smallest attenuation, and the highest attenuation was observed by sample 2 where the cells were treated thermally, this effect might be caused by the bound/unbound

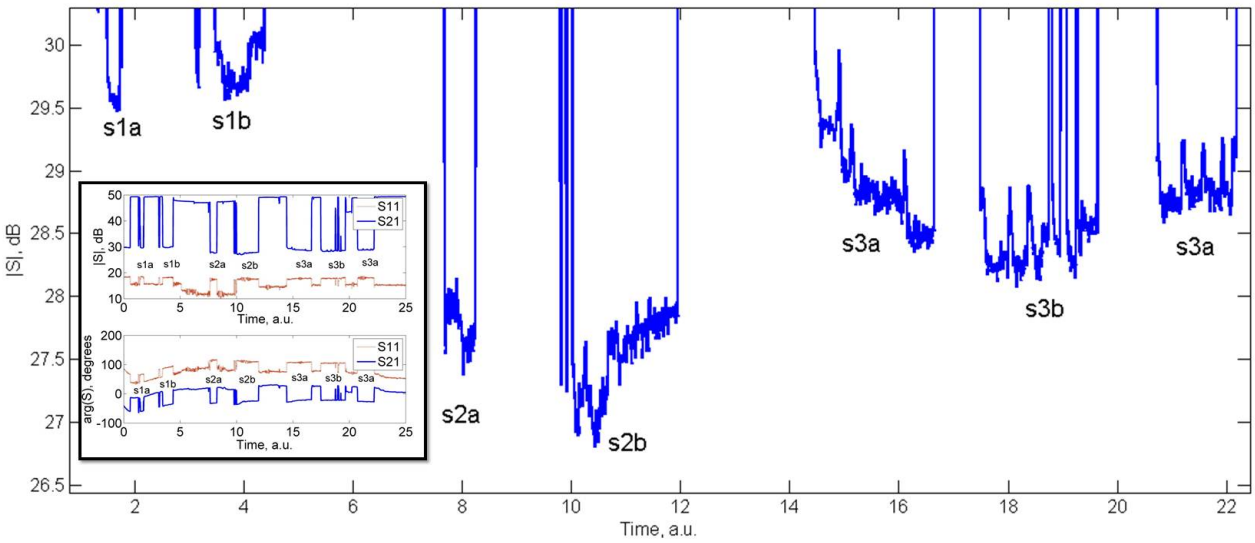

Fig. 6. Time sweep transmission zoomed measurement results at 275 GHz on the *S. cerevisiae*, inset overview of the S-parameters.

water molecules ratio change which results in observable contrast. For heat treated cells, the plasma membrane integrity is destroyed, which results in freely diffusion of small molecules from the cell. As expected, under an optical microscope with the $\times 100$ magnification no clear difference in structure or shape of the cells was observed except the treated cells seemed to be a bit smaller (might be a coincidence). To evaluate our method and perform quantitative evaluation of dead/living cells dyeing has to be performed.

The lower transmission signal level and thus smaller S/N ratio are result of the WH being by 1/5 bigger than required for good WR-WH transition. The intention was to produce slightly larger waveguide in order to simplify the alignment procedure, but precise and repeatable mechanical connection must be made for further studies. The wave propagating along the waveguide is partially reflected, transmitted (impedance mismatch) and absorbed at the CT. The LUT and THz-wave interaction does not happen efficiently, due to the standing wave generated with the maximum of the E-field being outside of the CT. The sensitivity increases only slightly with larger internal CT diameter. This is principal limitation of this WH&CT configuration and the significant improvement can be achieved with the capillary centered in a resonator, where the maximal oscillating E-field would be in the center of CT.

V. Conclusions

The hexagonal waveguide loaded with the capillary tube proved to be sensitive to the dielectric permittivity changes of the liquid under test contained within the capillary. The resulting S-parameter changes are not yet significant, but they prove the application possibility for this technology to detect μ-gravity influences on cell growth. More advanced sensor structures are under development aiming to increase the sensitivity with orders of magnitude.

References

[1] A. G. Markelz, "Terahertz dielectric sensitivity to biomolecular structure and function," *IEEE J. Sel. Top. Quant.*, vol. 14, no. 1, pp. 180–190, JAN-FEB 2008.

[2] S. E. Van Mulders, C. Stassen, L. Daenen, B. Devreese, V. Siewers, R. G. E. van Eijsden, J. Nielsen, F. R. Delvaux, and R. Willaert, "The Influence of Microgravity on Invasive Growth in Saccharomyces cerevisiae," *Astrobiology*, vol. 11, pp. 45–55, Jan. 2011.

[3] V. Matvejev, C. De Tandt, W. Ranson, and J. Stiens, "Wet silicon bulk micromachined THz waveguides for low-loss integrated sensor applications," in *2010 35th International Conference on Infrared, Millimeter, and Terahertz Waves (IRMMW-THz 2010)*. Piscataway, NJ, USA: IEEE, 2010 2010, Conference Paper, p. 2 pp., 2010 35th International Conference on Infrared, Millimeter, and Terahertz Waves (IRMMW-THz 2010), 5-10 September 2010, Rome, Italy.

[4] M. Asaki, A. Redondo, T. Zawodzinski, and A. Taylor, "Dielectric relaxation of electrolyte solutions using terahertz transmission spectroscopy," *J. Chem. Phys.*, vol. 116, no. 19, pp. 8469–8482, MAY 15 2002.

[5] M. Machado, S. Janssens, H. Soares, and E. Soares, "Removal of heavy metals using a brewers yeast strain of saccharomyces cerevisiae: advantages of using dead biomass," *J. Appl. Microbiol.*, vol. 106, no. 6, pp. 1792–1804, 2009. [Online]. Available: http://dx.doi.org/10.1111/j.1365-2672.2009.04170.x

[6] E. WALTON and J. PRINGLE, "Effects of Growth Temperature Upon Heat Sensitivity in Saccharomyces-Cererisiae," *Arch. Microbiol.*, vol. 124, no. 2-3, pp. 285–287, 1980.